Applied Surface Science 336 (2015) 143–149

Contents lists available at ScienceDirect

Applied Surface Science

journal homepage: www.elsevier.com/locate/apsusc

Comparison of laser ablation with spark discharge techniques used for nanoparticle production

Andrey Voloshko*, Jean-Philippe Colombier, Tatiana E. Itina

Laboratoire Hubert Curien, UMR CNRS 5516/Université de Lyon, Bat. F, 18 rue du Prof. Benoit Lauras, 42000, Saint-Etienne, France

ARTICLE INFO

Article history:
Received 3 July 2014
Received in revised form 15 October 2014
Accepted 15 October 2014
Available online 24 October 2014

Keywords:
Plasma processes
Nanoparticle formation
Numerical modeling

ABSTRACT

Based on numerical modeling, we compare laser ablation and spark discharge as promising methods of nanoparticle formation. First, we consider spark discharge between parallel plate metal electrodes. Second, we investigate nanosecond laser ablation of a metal target. For both phenomena copper is chosen to be nanoparticle material and argon at atmospheric pressure is used as an ambient gas. Despite different energy inputs, both differences and similarities are revealed in the corresponding plasma properties. The time-evolution of the critical particle sizes are, however, found to be similar in both cases.

1. Introduction

Both spark discharge [1–8] and nanosecond laser ablation [9–17] are used for nanoparticle (NP) production. The produced NPs have found numerous applications in such areas as electronics, biomedicine, textile production etc. Previous studies provide us information about the amount of NPs, their size distribution and possible applications. Particularly, it is shown that the main advantage of laser ablation method is the possibility of depositing stoichiometric multicomponent films [18–20], whereas spark discharge allows one to produce a large amount of nanoparticles in the aerosol state [1,2,21]. However, additional studies based on a more detailed comparison of both methods are required for the determination of similarities and differences of the NP properties.

Herein, we present the results of a detailed modeling of spark discharge and compare them with the ones obtained during nanosecond pulsed laser irradiation. Numerical modelling of spark discharge consists of several steps that are realized separately because of the difference in the corresponding time scales: (i) streamer formation and propagation between electrodes; (ii) streamer-to-spark transition; (iii) gas heating and cylindrical expansion, (iv) electrode evaporation and erosion; (v) nanoparticles formation. Typical models of nanosecond laser ablation also consist of several stages: (i) laser heating of the surface; (ii) evaporation of the surface; (iii) absorption of part of laser power by evaporated material; (iv) hemispherical expansion of target material; (v) nanoparticle formation. In this work, we focus our attention at the two last stages, since they provide nanoparticle properties, whereas the first three are described here in a simplified way. These assumptions are justified by the main objective of the study that is to compare NP formation processes in spark discharge and in laser ablation. In particular, we compare the roles of such processes as nucleation-controlled and diffusion-controlled primary NP formation for the two considered techniques.

2. Modeling details

2.1. Spark discharge

A typical set-up of spark discharge consists of two electrodes connected to the charged capacitance. The process starts by streamer formation. As soon as a high voltage V_0 is applied, initial electrons that are present in the gas start moving toward the anode. If voltage is high enough, the electrons gain enough energy from the electric field for collisional ionization of ambient gas atoms. The newly created electrons also start moving toward the anode, while the ions move toward the cathode. Because of the difference in masses, electron velocity is much higher and is gained much faster than the one of ions, so that ions are considered to be at rest during the streamer propagation. Electrons are deposited at the anode and, in turn, ions form a positive volume charge. This charge increases the local electric field $\vec{E}$ in the direction of the streamer propagation and decreases the one in the direction of the anode inside the streamer. Electrons gain more energy from

* Corresponding author. Tel.: +33 652731965.
E-mail address: andrey.voloshko@univ-st-etienne.fr (A. Voloshko).

http://dx.doi.org/10.1016/j.apsusc.2014.10.077
0169-4332/

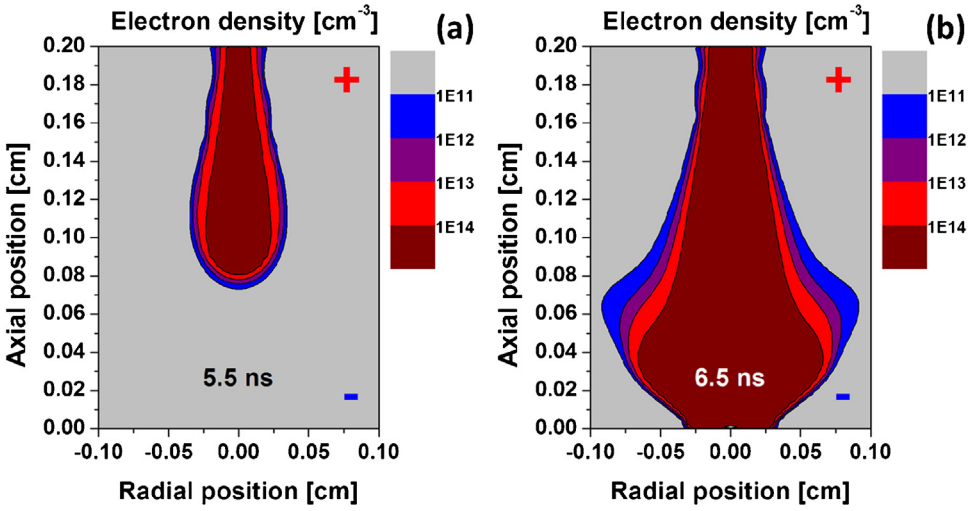

Fig. 1. Electron density in a typical streamer obtained for the delays of a) 5.5 ns; b) 6.5 ns. Here, gap distance is $d = 2$ mm, the applied voltage is 3.5 kV. Axial and radial positions correspond to z and r coordinates respectively.

the increased field, so that ionization becomes more efficient. As a result, the ionization area expands against electron motion until it reaches the cathode. This process is described numerically by using a system of drift-diffusion equations together with Poisson equation for electric potential V [22] and a set of boundary conditions as follows:

$$\frac{\partial n_e}{\partial t} + \left(\vec{\nabla} \cdot \vec{j}_e\right) = S, \tag{1}$$

$$\frac{\partial n_+}{\partial t} = S, \tag{2}$$

$$\vec{j}_e = -D_e \vec{\nabla} n_e - \mu_e n_e \vec{E}, \tag{3}$$

$$\Delta V = -\frac{e}{\varepsilon_0}\left(n_+ - n_e\right), \ \vec{E} = -\vec{\nabla} V, \tag{4}$$

$$V\big|_{z=0} = 0, \ V\big|_{z=d} = V_0, \ \left.\frac{\partial V}{\partial r}\right|_{r=0} = 0, \ V\big|_{r=r_{\max}} = V_0 \frac{z}{d}, \tag{5}$$

where z and r are coordinates of the used cylindrical coordinate system with $z = 0$, $z = d$, $r = 0$ and $r = r_{max}$ corresponding to the position of the cathode surface, of the anode surface, of the center of symmetry of the discharge and of the distant surface respectively; n_e and n_+ are electron and ion densities respectively; j_e is electron density flux; S is the ionization density rate; D_e and μ_e are the electron diffusion and mobility coefficients respectively; e is the electron charge, and ε_0 is the vacuum permittivity. For instance, calculations performed by using Eqs. (1)–(5) give a breakdown voltage of ~3.5 kV and the time of streamer propagation is of ~6.5 ns for copper electrodes in argon at 1 atm pressure, and for the gap of 2 mm (Fig. 1).

When the streamer reaches the opposite electrode, electron emission increases dramatically, so that the streamer is transformed in a conductive plasma column. The discharging circuit is commonly described by an RLC-circuit with an equivalent resistance instead of the plasma column. Previous experiments reveal [23] that discharging of the capacitance C oscillates, resulting from the inductance L of used cables. The behavior of the electric charge Q in the corresponding circuit with the total resistance R_Σ is described by the Kirchhoff's voltage law for RLC-circuit [24] as follows:

$$L\frac{d^2Q}{dt^2} + R_\Sigma \frac{dQ}{dt} + \frac{Q}{C} = 0. \tag{6}$$

An under-damped solution for the electric current I is derived from Eq. (6) under the conditions of $R_\Sigma{}^2 \ll 4L/C$ is

$$I \approx -V_0\sqrt{C}\frac{4L + R_\Sigma{}^2 C}{L^{\frac{3}{2}}} \sin\left(\frac{t}{\sqrt{LC}}\right) \exp\left(-\frac{R_\Sigma}{2L}t\right). \tag{7}$$

The oscillating behavior of the discharge is presented in Fig. 2, defining the properties of the following plasma column. According to this solution, both electrodes play a role at different delays leading to both evaporation and erosion of the electrodes. Each time after the polarity switches, a crater is formed on the surface of one of the electrodes due to both evaporation and erosion. We suppose each new evaporation/erosion event independent from previous. Thus we are able to calculate all the evaporation/erosion that takes place on the cathode surface as it is discussed further. To evaluate the total amount of evaporated/eroded material from both electrodes, we multiply the result by 2.

We suppose plasma to be homogeneous in z direction except in a thin cathode layer [25] as it is shown in Fig. 3. This assumption is justified during most of the plasma column expansion stage considered here.

We consider that electrode material erosion flux density j^{Σ}_{surf} consists of two main processes: (i) thermal evaporation caused by Joule heating, and (ii) sputtering due to ion bombardment. Thermal evaporation material flux density j^{T}_{surf} is described by thermal

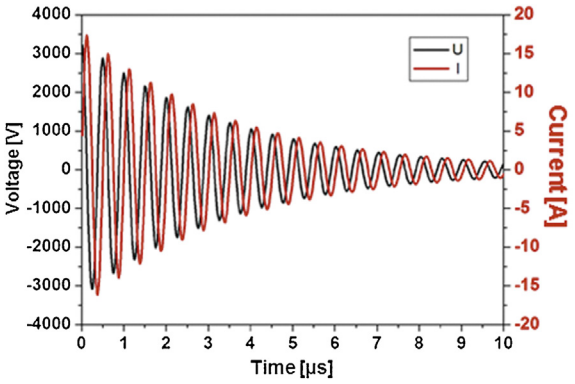

Fig. 2. Typical time evolutions of voltage and electric current during a "single" spark event, obtained for $V_0 = 3.5$ kV; $C = 0.15$ nF; $L = 50$ μH; $R_\Sigma = 30$ Ω.